RSC Advances

ROYAL SOCIETY OF CHEMISTRY

www.rsc.org/advances

Exploring optoelectronic structure and thermoelectricity of recent photoconductive chalcogenides compounds $CsCdInQ_3$ (Q = Se, Te)

Wilayat Khan[1,*] and Souraya Goumri-Said[2,†]

[1] New Technologies – Research Center, University of West Bohemia, Univerzitni 8, Pilsen 306 14, Czech Republic

[2]School of Chemistry and Biochemistry and Center for Organic Photonics and Electronics, Georgia Institute of Technology, Atlanta, Georgia 30332-0400, United States

Abstract

The photoconductive quaternaries, $CsCdInQ_3$ (Q = Se, Te), have been synthesized recently and have shown to be potential materials for hard X-ray and γ-ray detection. These materials have relatively high densities and band gap in range of 1.5−3 eV, which make them fulfilling the requirement of hard detection devices. In the present work, we investigate the metal chalcogenide $CsCdInQ_3$ as deduced from a full potential linearize augmented plane wave method based on density functional formalism. The direct band gap is estimated at level of EVGGA functional, as 2.11 and 1.75 eV for $CsCdInSe_3$ and $CsCdInTe_3$ respectively. These values are in good agreement with the experimental measurements (2.40 and 1.78 eV) performed from solid-state UV−vis optical spectroscopy. Optical parameters including the dielectric constant, absorption coefficient, energy loss function reflectivity and refractive index are also reported to investigate the potential role of these metal chalcogenide compounds for solar conversion application. Our calculated optical band gap is compared to the measured experimental values on a Lambda 1050 UV−vis-IR spectrophotometer in the range of 300−1500 nm. The thermoelectric properties discuss the variation of the electrical and thermal conductivity, Seebeck coefficient and power factor with the temperature variation, using Boltzmann transport theory.

Key words: metal chalcogenide, photo-induction, thermoelectric properties, DFT

Corresponding authors: * walayat76@gmail.com (W. Khan)

†Souraya.Goumri-Said@chemistry.gatech.edu (Souraya Goumri-Said)

I. Introduction

The increase demand on new compounds, for imaging and detection capable of detecting hard X-ray and γ-rays, have led to conduction of intensive research on semiconductors in material science engineering and also chemistry disciplines. Semiconductors are good detectors because they have a good energy resolution and the facility to fabricate compact arrays compared to other inorganic scintillation detectors [1, 2].

The photoconductive semiconductors have shown to be a promising alternative to the expensive silicon in both forms polycrystalline and amorphous [3-5]. These latter are having a low stopping power for high energy photons, which is limiting their application to hard X-ray and γ-rays. Furthermore, germanium has a small band gap that requires operating at cryogenic temperatures to have detection activity [6]. Consequently, room-temperature semiconductors with high atomic numbers and wide band gaps are highly recommended to overcome all limitations of Silicon and Germanium. Most importantly, the wide band gaps semiconductors have been long under development to make materials useful for medical and industrial imaging systems as well as designing new detectors for high energy particle- and astrophysics [6].

Chalcogenides are potential candidates for hard detection because of their wide band-gap, good electro-transport properties and high resistivity. Since early seventies, chalcogenides such as Cadmium Telluride (CdTe) has been considered as promising semiconductor materials for hard X-ray and γ -ray detection. However, compared to Si and Ge, CdTe is hard to use for nuclear spectroscopy due to its poor spectroscopic performance and lack of stability. In order to overcome CdTe limitation, research on discovery of new chalcogenides with wide band gap is growing exponentially. In fact, these materials are known to become more electrically conductive due to the absorption of electromagnetic radiation such as visible light, ultraviolet light, infrared light, and even gamma radiation [8]. Photoconductive materials include a large variety of materials and structures such as the conductive polymer polyvinylcarbazole [9] used extensively in photocopying (xerography); lead sulfide, used in infrared detection applications [10].

In general, metal chalcogenides are compounds made from a metallic element and a member of the chalcogenide family, namely the elements under oxygen–sulfur, selenium, and tellurium. These materials are used for various applications such as: solar energy conversion and solar cells, semiconducting metal chalcogenide aerogels, Infrared detection for optoelectronics, non-linear optics, thermoelectrics, hard detection and energy conversion [8-10]. The three latest

applications are the scope of the present work, where we report results of *ab-initio* approaches investigations of optoelectronic and thermoelectric properties of the quaternary $CsCdInQ_3$ (Q = Se, Te). In fact, $CsCdInQ_3$ (Q = Se, Te) has been subject of experimental and theoretical studies performed by Hao Li *et al.* [11], where they synthesized the metal chalcogenides using a polychalcogenide flux technique. In addition to materials synthesis, the authors determined that these materials are having a layered structure within a monoclinic symmetry. The reported measured electronic band gaps were found direct and large enough to be potentially interesting for hard radiation detection applications. The optical band gap was measured using ground crystals and the absorption spectra from solid-state UV−vis optical spectroscopy. The performed density functional theory (DFT) calculations on these compounds have shown the limitation of the employed functional, the generalized gradient approximation (GGA) [12], to determine the exact band gap values, and perform a detailed comparison between both chalcogenide. These materials are layered systems where the dimensionality reduction plays an important role in tuning their band gap. This interesting behavior is making $CsCdInQ_3$ (Q = Se, Te) band gap tuning possible for hard detection devices and thermoelectric conversion application. Furthermore, due to huge demand on alternative materials for energy conversion and PV application, we extend our investigation to the thermoelectric properties by calculation of Figure of merit using Boltzmann transport theory [13] combined to density functional theory (DFT) outputs. The calculation of the optoelectronic and thermoelectric properties, using an improved computational tool, led us to understand the effect of structure/dimension perturbations on the band gap and related optical and thermoelectric properties. These finding will help experiments to find a desirable ways to tune the electronic structures of $CsCdInQ_3$ (Q = Se, Te) .

II. Structure description and computational details

$CsCdInQ_3$ (Q = Se, Te) are considered as layered structure and crystallize in the monoclinic space group C2/c. The structure of $CsCdInTe_3$ as shown in Fig. 1, is iso-structurally analogous to $CsCdInSe_3$ but a slight difference occur for the five Cd^{2+} and In^{3+} sites were they are having a mixed occupancy [11]. The valence sum for Cd^{2+} is around 2.25 whereas for In^{3+} it is evaluated to 3.20. From crystallography consideration and following the experimental measurement [11], a typical structure is displayed in Fig. 1.

In order to study the properties like energy band structures, total and partial density of states and optical properties of $CsCdInTe_3$ and $CsCdInSe_3$ were carried out using the full potential linearized augmented plane wave method (FP-LAPW) as employed in the computation package (WIEN2k) [14] in the field of DFT. In FP-LAPW method, the unit cell is decomposed into (1) muffin tin (MT) sphere (non-interacting) and (2) interstitial region. We have implemented the Monkhorst–Pack *k*-point mesh of $16\times5\times16$ in the irreducible Brillouin zone (IBZ) for the self-consistent calculations. For the optimization of the structure, the generalized gradient approximation (GGA) [12] was used while the Engel Vosko generalized gradient functional (EVGGA) [15] was used for the optical properties. For the self-consistent computation, both total energy and charge of the compounds are relaxed upto 0.00001 eV and 0.0001 eV, respectively. The entire basis sets i.e. Cs (6s, 5p, 4d), Cd (5s, 4p, 4d), In (5s, 5p, 4d), Se (4s, 4p, 3d) and Te (5s, 5p, 4d) were studied by using the down-folding methods [16].

BoltzTraP code [13] was also used to calculate the entire transport coefficients under constant scattering time of the crystalline materials on the basis of Boltzmann transport theory [13] and the rigid band approach, which effectively explained the electronic structure and transport coefficients of numerous compounds. In these calculations, we ignore the temperature dependence on E-K curve (energy band structure). Using the above approaches, except the Seebeck coefficient (S) the remaining transport coefficients i.e. electrical conductivity(σ), thermal conductivity(κ_{ele}), power factor $(S^2\sigma)$ can be calculated with constant relaxation time(τ).

III. Optoelectronic properties

The calculated band structures (BS) and density of states (DOS) are displayed in Fig. 2(a) and (b) for $CsCdInSe_3$ and $CsCdInTe_3$ respectively. Their band gaps are direct and are found 2.11 eV and 1.78 eV from EVGGA functional. These values are almost in good agreement with the experimental measurement found 2.40 and 1.75 eV for $CsCdInSe_3$ and $CsCdInTe_3$ respectively. Our calculated band gap values are closest to the experimental values measured with diffuse reflectance as found equal to 1.81 eV for $CsCdInTe_3$ and somehow good compared to the measured band gap of 2.17 eV for $CsCdInSe_3$. A deep research in these compounds is showing that other measurements based on diffuse reflectance and absorption method [11] are

giving band gaps of 2.17 eV for CsCdInSe3 and 1.75 eV for $CsCdInTe_3$. We can see that our calculations are in better agreement with these later measurements than the first method reported in [11]. Furthermore, this finding proves that the discrepancy observed between our calculation and experimental band gap is not related to the employed method, EV-GGA (actually the most robust in band gap calculation). Furthermore, the first theoretical study dealing with these chalcogenides was performed on the level of semilocal approximation like GGA [11], have revealed a direct band gap of 1.53 eV (I) and 1.39 eV (II) at the Γ-point, which are underestimated compared to the experimental band gaps. To correct these calculations, the authors have suggested performing more exact methods such as screened exchange LDA [17], GW approximation [18], or hybrid functional [19]. From our investigation, we show that EV-GGA [12] is sufficient to reproduce the right band gap extracted from the optical measurements.

The projected densities of states (PDOS) calculations of $CsCdInQ_3$ (Q = Se, Te) are showing, in Fig. 2(a) and (b) that the valence band maxima (VBM) are mainly composed of Se(Te) 4p(5p)-orbitals. Cd 4d-orbitals contribute to a much lesser extent to the VBM and the conduction band minima (CBM) consist of hybridization bands made up of Se(Te) 4p(5p)-orbitals and In 5s-orbitals.

Before turning our attention to the optical properties, it is important to notice that the decrease of the measured and even calculated band gap values from the initial chalcogenides compounds, can be explained using the "concept of reduction" and "dimensional reduction" introduced in II-VI materials [20] and more recently in designing new radiation detection materials such as the alkali metal chalcogenide [21]. In fact, it was proven that compounds containing very high Z elements such as the binary Hg-based binary chalcogenides can lead to a ternary compounds with high bandgap (>1.6 eV) with high resistivity and specific density. For the present compounds, the insertion of [CdQ] layers into the $CsInQ_2$ structure form $CsCdInQ_3$ with a dimensional increase (i.e. a band gap decrease) compared to the initial compound $CsInQ_2$ leading to suitable band gap for X-ray and γ-ray detection.

Given the stability and apparent broad range of the of $CsCdInQ_3$ electronic structure type, we expect further to tune the optical band gaps by changing Q as Se or Te. We display in Fig.3 (a), (b) and (c), the real and imaginary part of the dielectric constants ($\varepsilon_1(\omega)$ and $\varepsilon_2(\omega)$), the

absorbance coefficient $I(\omega)$, energy loss function $L(\omega)$, respectively. We have calculated the imaginary part $\varepsilon_2(\omega)$ using EV-GGA potential (Fig. 3(a, b)). From $\varepsilon_2(\omega)$ plots, we analyzed that the threshold energy (critical point) occurred at 2.11 and 1.75 eV respectively for is corresponding to band gap of $CsCdInSe_3$ and $CsCdInTe_3$ respectively. At this critical point optical transitions between valence band maximum and conduction band minimum are direct as it is deduced from the band structures. The existence of an abrupt increase in the curve beyond this energy is due to the occurrence of more inter-band transitions.

There are also prominent peaks in $\varepsilon_2(\omega)$ of $CsCdInTe_3$ as well as for to $CsCdInSe_3$ compound that have maximum magnitude among other components occurred at around 4 and 5.8 eV for $CsCdInTe_3$ and at 5 and 6.3 eV $CsCdInSe_3$. These maximum peaks are caused by the electric dipole transitions between valence and conduction band. The magnitude of $\varepsilon_2(\omega)$ is constantly decreasing at higher energies for both compounds. At intermediate energies maximum anisotropy exist among the three components of dielectric constant. At this stage of calculation, we use Kramers-Kronig relation [22] to extract the real part $\varepsilon_1(\omega)$of dielectric function from the imaginary part using $\varepsilon_1(\omega)=1+\frac{2}{\pi}p\int_0^{\infty}\frac{\omega'\varepsilon_2(\omega')}{\omega'^2-\omega^2}d\omega'$ (Were P is the principal value of integral). Calculated real part $\varepsilon_1(\omega)$ of dielectric function for $CsCdInQ_3$ are displayed in Fig.3. The maximum peak of magnitude 8.6 (a.u) is located at around 2.25eV for $CsCdInTe_3$ and at 6.6 (a.u) at 3.1 eV for $CsCdInSe_3$. It is important to remind here that we have only calculated the electronic contribution since both the electrons and ions contribute to the dielectric constant of compounds. Furthermore, static dielectric constant values are found equivalent to 6, and 4.8 for $CsCdInTe_3$ and $CsCdInSe_3$, respectively. In Fig.3c, we display the absorption coefficient $I(\omega)$ as calculated using EV-GGA, absorption spectrum is starting at 2.0 eV for both chalcogenides and has attained a maximum value at about 7.0 and 7.8 eV for $CsCdInTe_3$ and $CsCdInSe_3$, respectively. Beyond this energy region, absorption curves decrease then they start to increase. From the dielectric constants, we can determine the energy loss function $L(\omega)$ as $L(\omega)=\mathrm{Im}\left(-\frac{1}{\varepsilon(\omega)}\right)$. These functions as displayed in Fig. 3d are useful for providing useful information about the electronic systems interacting with incident electron beam. For both chalcogenides, our ELF show broad spectrum in the energy range 2.0-14.0 eV. The significant

feature about $L(\omega)$ is that the main peaks represent the characteristics plasma resonance occurring at plasma frequency corresponding to energy (12.0 eV for $CsCdInTe_3$ and 12.2 for $CsCdInSe_3$). At this point of energy, the reflectivity spectrum shows a sudden reduction in the curve as is shown in Fig. 3e. For both chalcogenides, these curves show that the reflectivity increases with energy and reaches a maximum value of 70% at around 13.5 eV. Reflectivity is found to be 15 %, (17 %) for $CsCdInTe_3$ ($CsCdInSe_3$) at zero vibration, the valleys in the reflectivity spectrum correspond to the peaks in the energy loss function of Fig. 3d. For both compounds, we have also calculated refractive index $n(\omega)$ in Fig. 3f. Refractive indices increase with energy in the lower energy region and reached maximum values at 2.8 and 3.5 eV for $CsCdInTe_3$ and $CsCdInSe_3$ respectively.

IV. Thermoelectric properties

The temperature dependent electrical conductivity, thermal conductivity, Seebeck coefficient, power factor and ZT for both $CsCdInTe_3$ and $CsCdInSe_3$ compounds are displayed in Fi. 4. These properties are responsive to the energy band gap values. As for the experimental one, our found band gaps are direct and show a variation with temperature induced by the thermal excitation of electrons. On the basis of calculated energy band structure and density of states, one can easily calculate the electrical conductivity, σ^{ave} , under constant relaxation time as a function of temperature. Fig 4a, shows a linear increase of the electrical conductivity (σ^{ave}) of both compounds $CsCdInSe_3$ and $CsCdInTe_3$ when temperature increase from 100 to 800 K. σ^{ave} is growing up due to the excitation of the carrier from the valence band to the conduction band when the temperature increases, and induces an increase of the number of carrier concentrations devoted to conduction. The $CsCdInSe_3$ depicts low electrical conductivity at small carrier concentration up to 350 K but beyond this temperature σ^{ave} increases compared to $CsCdInTe_3$. The behavior of the σ^{ave} might be inter-related to the valence shell electronic configuration of Se and Te atoms. The lattice and electronic parts contribute to the total thermal conductivity and each change differently with temperature. In the theoretical model, we ignore the lattice thermal conductivity κ_{lat} and pay attention to electronic part of the thermal conductivity κ_{ele}. Thermal conductivity is directly varying with the following parameters: (i)

carrier concentration (ii) electrical conductivity and (iii) mobility of the carrier i.e. $\kappa_e = \sigma\mu n$. The electronic thermal conductivity κ_{ele} of $CsCdInSe_3$ and $CsCdInTe_3$ compounds is $3.15\times10^{14} W/mKs$ at low temperature (100 K) and $2.18\times10^{14} W/mKs$ for $CsCdInSe_3$ and $2.22\times10^{14} W/mKs$ for $CsCdInTe_3$ at high temperature (800 K). Fig 4b shows linear increase in the thermal conductivity κ_{ele} of both compounds when temperature enhances from 100 to 800 K. Thermal conductivity κ_{ele} of $CsCdInSe_3$ is greater than $CsCdInTe_3$ and mainly originated from the electronic part.

Fig 4c represents the computed Seebeck coefficients S^{ave} under the temperature ranging from 100 to 800 K at different doping materials. The calculated Seebeck coefficients of both compounds are strongly depending on the temperature and carrier concentration, where we can see an inverse relation of the carrier concentration and Seebeck coefficients [23]. It is clear from Fig 4c that both compounds ($CsCdInSe_3$ and $CsCdInTe_3$) are p-type compounds. The S^{ave} of $CsCdInSe_3$ shows an abrupt increase with temperature up to 250 K, while in $CsCdInTe_3$ the Seebeck coefficient enhances steadily with temperature up to 450 K and indicate stability between 450 to 600 K. Beyond 250 K, it decreases due to the increases of the carrier concentration and temperature (in $CsCdInSe_3$). At higher value of temperature (at 800 K), both compounds show dispersive nature i.e. the value of the Seebeck coefficient is reaching 180 $\mu V/K$ for $CsCdInSe_3$ and 183 $\mu V/K$ for $CsCdInTe_3$. One can also observe a very small decrease in the value of S^{ave} in $CsCdInTe_3$ with the increase of the temperature than in case of $CsCdInSe_3$. These findings confirm the dependence of S^{ave} on temperature and carrier concentration changes. One can see from the energy band structure (displayed in Fig. 2a) that bands are less dispersive around the Fermi level and at lower energy, so the effective mass values will be smaller for the correspond fundamental particles i.e. electrons and holes, leading to smaller value of Seebeck coefficient. Furthermore, both compounds have different dispersion in their bands, which are also responsible on the change in the magnitude of the Seebeck coefficients.

The power factor $S^2\sigma$ shown in Fig 4d can be calculated from the thermoelectric power and electrical conductivity. For an increase in temperature, from 100 to 800 K, $S^2\sigma$ increases from

0.30 to $2.12\times10^{11} W/mK^2 s$ for $CsCdInSe_3$ and reaches a value of $1.97\times10^{11} W/mK^2 s$ for $CsCdInTe_3$. In addition, one can have a maximum power factor by replacing Te on Se. It means that $CsCdInSe_3$ has the larger carrier concentration compared to $CsCdInTe_3$. The calculated power factors of both p-type compounds rapidly increases due to the increase in carrier concentration with the increase in temperature. The increase in electrical conductivity is responsible for the greater value of power factors. These findings confirm that $CsCdInSe_3$ is more suitable for thermoelectric devices than $CsCdInTe_3$, because its thermoelectric properties can be enhanced effectively at high temperature.

Combining the electrical conductivity and Seebeck coefficient time's temperature over thermal conductivity, the figure of merit i.e. $ZT = S^2\sigma T/\kappa$ of both chalcogenides is shown in Fig 4e. It is clear from the Fig.4e, that the figure of merit (ZT) of both compounds show different behavior at low temperature, in particular from 100 to 350 K and then increases parallel with temperature beyond 350 K. Comparing these figures of merit (ZT) i.e. 0.75 for $CsCdInSe_3$ and 0.71 for $CsCdInTe_3$, one can easily conclude that the first compound is better than the second compound along the entire temperature interval. Fig.4e indicates that ZT is affected by two parameters: (i) temperature and (ii) doping element. Greater ZT are mainly originated from higher electrical conductivity and lower thermal conductivity. In addition, changes in values of (ZT) from 0.60 to 0.75 suggest that $CsCdInSe_3$ is very prominent material for both types of uses: cooling devices and thermoelectric applications, while $CsCdInTe_3$ can be used only in thermal devices. Most importantly, figures of merit of both compounds are showing a strong dependence on temperature.

V. Conclusion

In the present work, we investigated, using full potential linearize augmented plane wave method based on density functional formalism, metal chalcogenide $CsCdInQ_3$ (Q = Se, Te) in view of their potential implication in detectors devices for X-ray and γ-rays and thermoelectric devices. The optoelectronic properties are showing a direct band gap, estimated at level of EVGGA, 2.11 and 1.75 eV for $CsCdInSe_3$ and $CsCdInTe_3$ respectively. These finding agree well with solid-state UV−vis optical spectroscopy measurements (2.40 and 1.78 eV, respectively). Our computed optical band gap is compared to the measured experimental values on a Lambda

1050 UV−vis-IR spectrophotometer in the range of 300−1500 nm. Both of $CsCdInQ_3$ are showing interesting thermoelectric properties making them potentially candidates for cooling and thermal devices.

Acknowledgements

The work of W. Khan was developed within the CENTEM project, reg. no. CZ.1.05/2.1.00/03.0088, co-funded by the ERDF as part of the Ministry of Education, Youth and Sports OP RDI program. MetaCentrum and the CERIT-SC under the program Centre CERIT Scientific Cloud, reg. no. CZ.1.05/3.2.00/08.0144.

References

[1] Milbrath, B. D.; Peurrung, A. J.; Bliss, M.; Weber, W. J. J. Mater. Res. 2008, 23, 2561−2581

[2] Owens, A.; Peacock, A. Nucl. Instrum. Methods, A 2004 , 531,18−37

[3] Chung, D. Y.; Hogan, T.; Brazis, P.; Rocci-Lane, M.; Kannewurf, C.; Bastea, M.; Uher, C.; Kanatzidis, M. G. Science, 287, 1024 (2000).

[4] Hsu, K. F.; Loo, S.; Guo, F.; Chen, W.; Dyck, J. S.; Uher, C.; Hogan, T.; Polychroniadis, E. K.; Kanatzidis, M. G. Science, 303, 818 (2004).

[5] Pandey, A.; Brovelli, S.; Viswanatha, R.; Li, L.; Pietryga, J. M.; Klimov, V. I.; Crooker, S. A. Nat. Nanotechnol., 7, 792 (2012).

[6] M. Richter and P. Siffert, “High resolution gamma ray spectroscopy,” Nucl. Instr. Meth. , vol. A322, pp. 529-537, 1992.

[7] P. Siffert, “Cadmium telluride and related materials as X- and gamma-ray detectors: A review of recent progress,” Proc. SPIE , vol. 2305, pp. 98- 109, 1994

[8] DeWerd, L. A.; P. R. Moran "Solid-state electrophotography with Al_2O_3". *Medical Physics* **5** (1): 23–26 (1978).

[9] K. Y. Law, "Organic photoconductive materials: recent trends and developments". *Chemical Reviews, American Chemical Society* **93**: 449–486 (1993).

[10] Sootsman, J. R.; Chung, D. Y.; Kanatzidis, M. G. Angew. Chem., Int. Ed., 48, 8616 (2009).

[11] H. Li, C. D. Malliakas, J. A. Peters, Z. Liu, J. Im, H. Jin, C. D. Morris, L-D. Zhao, B. W. Wessels, A. J. Freeman, and M. G. Kanatzidis, Chem. Mater., 25, 2089−2099 (2013).

[12] Perdew JP, Burke K, Ernzerhof M (1996) Phys. Rev. Lett. 77:3865.

[13] G.K.H. Madsen, D.J. Singh, Comput. Phys. Commun. 175 67 (2006).

[14] Blaha P, Schwarz K, Madsen GKH, Kvasnicka D, Luitz J (2002) WIEN2K: an augmented plane wave plus local orbitals program for calculating crystal properties. Technische Universitat Wien, Vienna.

[15] E. Engel, S.H. Vosko, Phys. Rev. B 47 (1993) 13164.

[16] Lambrecht, W. R. L.; Andersen, O. K. Phys. Rev. B 1986, 34, 2439.

[17] A. Seidl, A. Görling, P. Vogl, J. A. Majewski, and M. Levy, Phys. Rev. B **53**, 3764 (1996).

[18] L. Hedin, Phys. Rev., 139 (1965), pp. A796–A823.

[19] A.V. Krukau, O.A. Vydrov, A.F. Izmaylov, G.E. Scuseria, J. Chem. Phys., 125 (22) (2006), p. 224106.

[20] Enos A. AxtellIII, Ju-Hsiou Liao, Zoe Pikramenou, and Mercouri G. Kanatzidis, Chem. Eur.J.1996, 2, 6.

[21] Androulakis, J.; Peter, S. C.; Li, H.; Malliakas, C. D.; Peters, J. A.; Liu, Z. F.; Wessels, B. W.; Song, J. H.; Jin, H.; Freeman, A. J.; Kanatzidis, M. G. Adv. Mater. 2011, 23, 4163

[22] R. de L. Kronig, *On the theory of the dispersion of X-rays,* J. Opt. Soc. Am., vol. **12**, p. 547-557 (1926).

[23] C. Stiewe, L. Bertini, M. Toprak, M. Christensen, D. Platzek, S. Williams, C. Gatti, E. Muller, B.B. Iversen, M. Muhammed, M. Rowe, J. Appl. Phys., 97 (2005), p. 044317

Figures caption

Fig.1: Structure of the metal chalcogenide $CsCdInQ_3$ (Q = Se, Te).

Fig.2: Calculated band structure, total and partial density of states of (a) $CsCdInSe_3$ and (b) $CsCdInTe_3$.

Fig.3: Calculated optical properties using EVGGA: (a) Imaginary part of dielectric function (b) Real part of dielectric function (c) Absorption coefficient (d) Energy loss function (e) Reflectivity and (f) Refractive index.

Fig. 4: Calculated thermoelectric properties as a function of temperature: (a) electrical and (b) Thermal conductivity, (c) Seebeck coefficient (d) power factor and (e) Figure of merit.

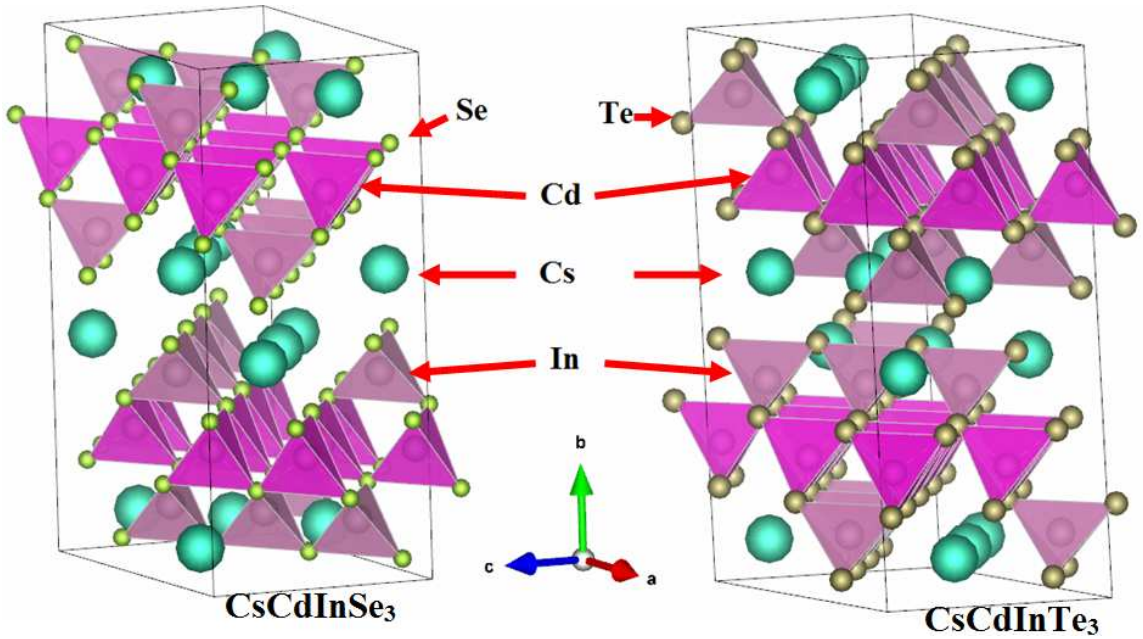

Fig.1

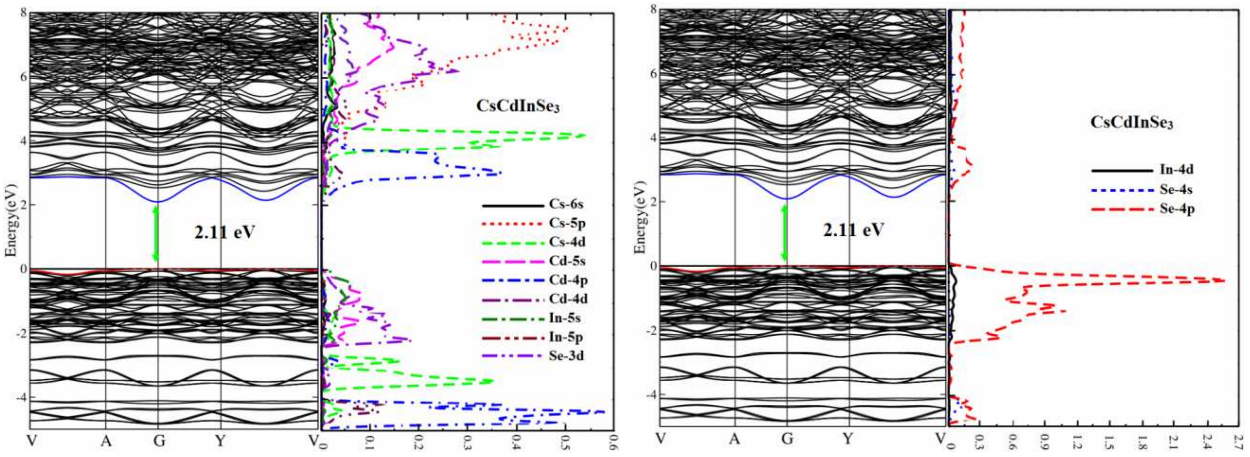

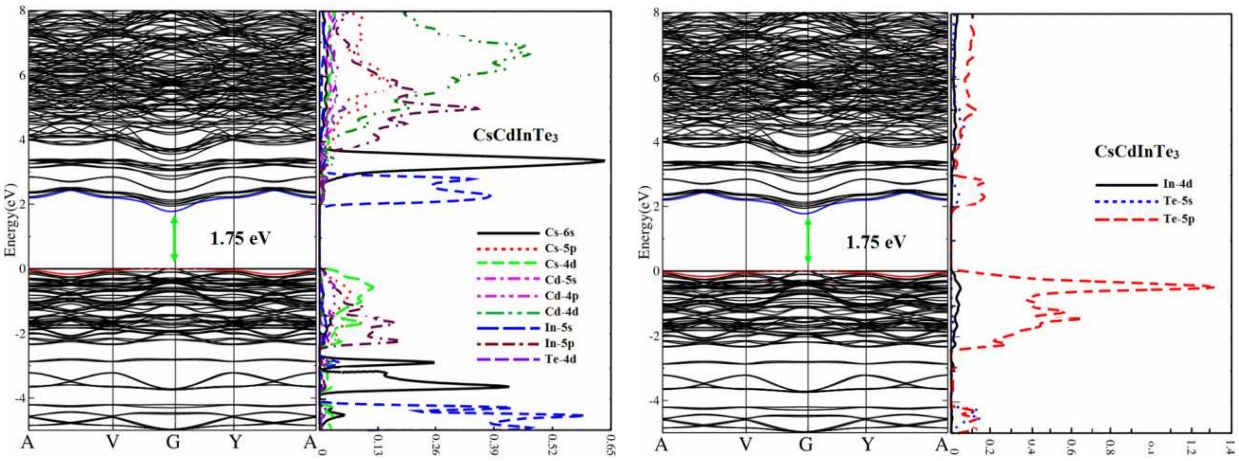

Fig.2(a) and (b)

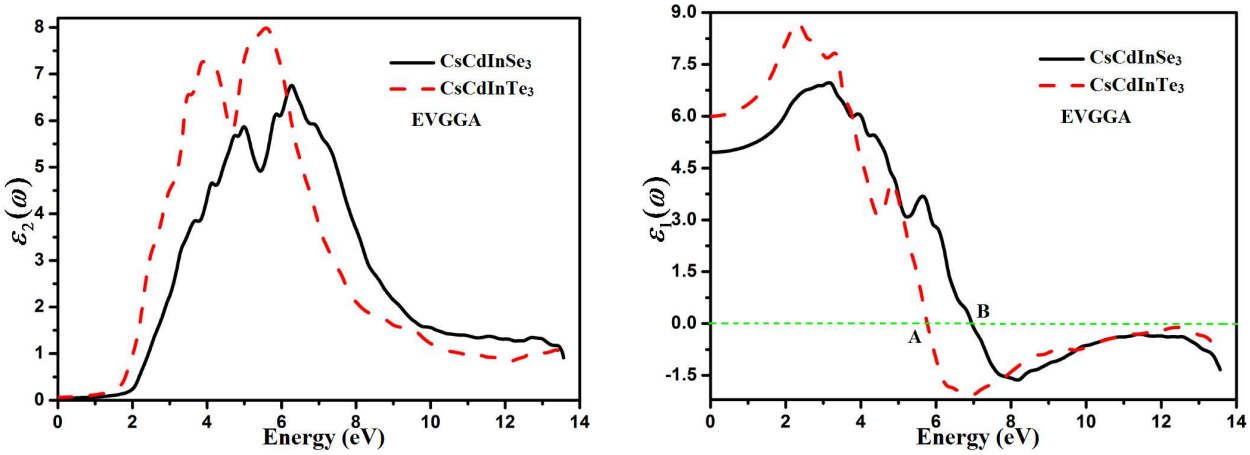

(a) **(b)**

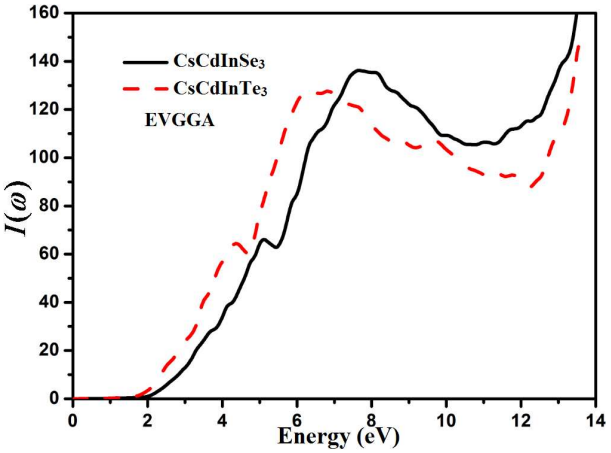

(c)

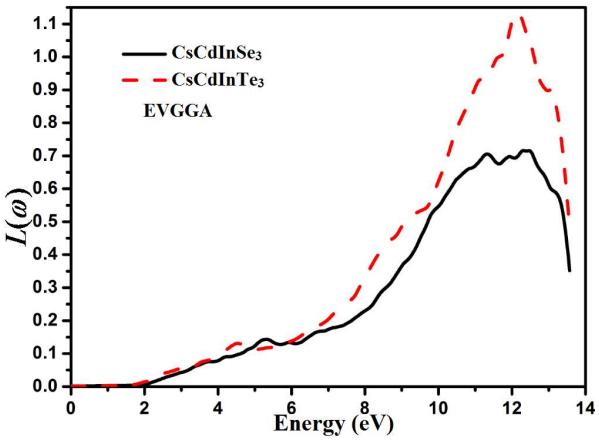

(d)

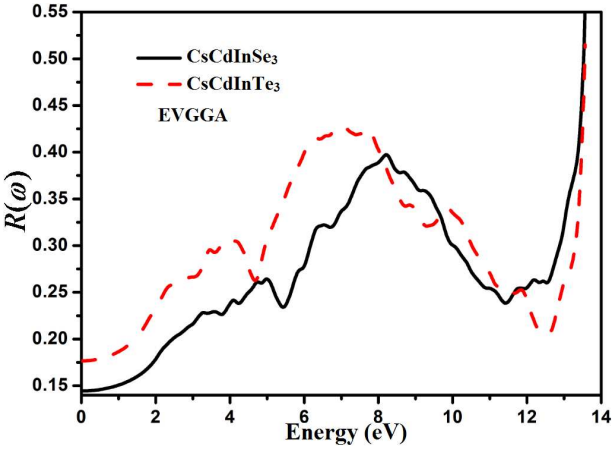

(e)

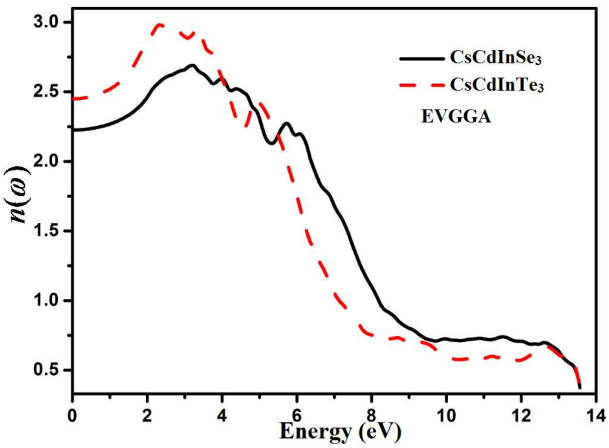

(f)

Fig. 3 (a), (b), (c), (d), (e) and (f)

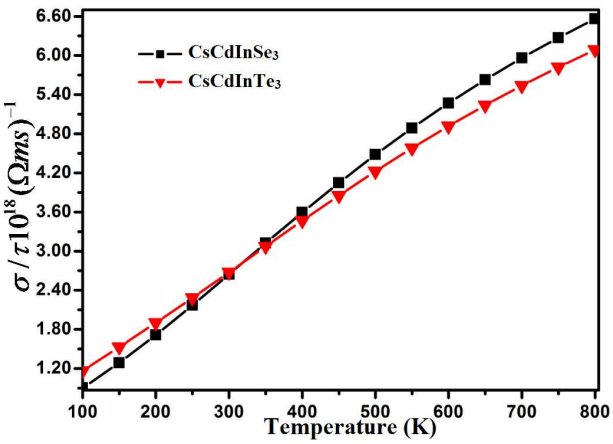

(a)

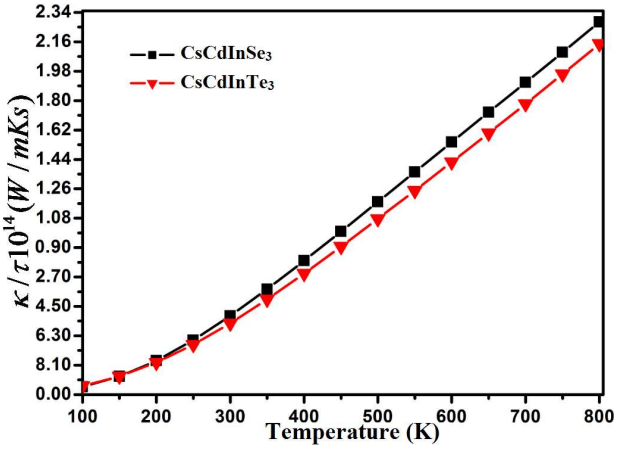

(b)

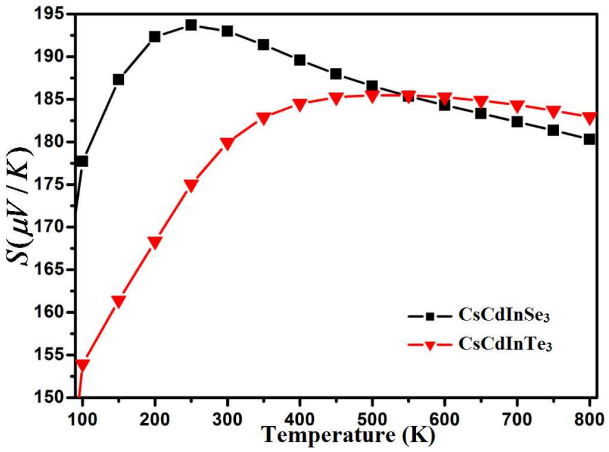

(c)

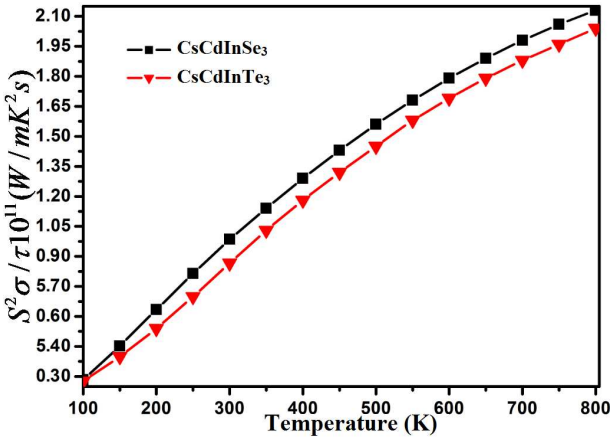

(d)

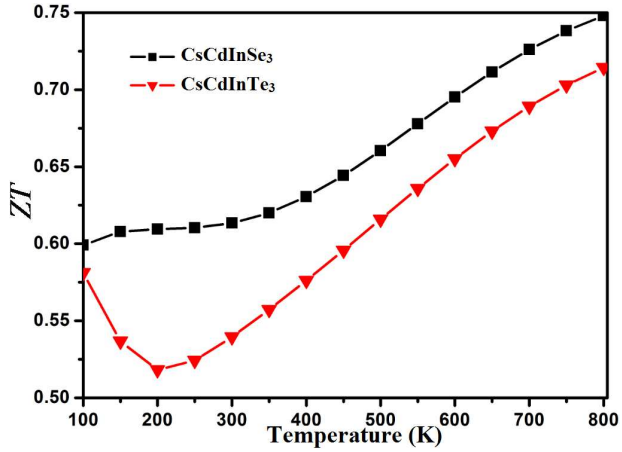

(e)

Fig. 4(a), (b), (c), (d), and (e)